

Transcriptome Analysis of CHO Cell Size Increase During a Fed-Batch Process

Xiao Pan, Abdulaziz A. Alsayyari, Ciska Dalm, Jos A. Hageman, René H. Wijffels, and Dirk E. Martens*

In a Chinese Hamster Ovary (CHO) cell fed-batch process, arrest of cell proliferation and an almost threefold increase in cell size occurred, which is associated with an increase in cell-specific productivity. In this study, transcriptome analysis is performed to identify the molecular mechanisms associated with this. Cell cycle analysis reveals that the cells are arrested mainly in the G_0/G_1 phase. The cell cycle arrest is associated with significant up-regulation of cyclin-dependent kinases inhibitors (CDKNs) and down-regulation of cyclin-dependent kinases (CDKs) and cyclins. During the cell size increase phase, the gene expression of the upstream pathways of mechanistic target of rapamycin (mTOR), which is related to the extracellular growth factor, cytokine, and amino acid conditions, shows a strongly synchronized pattern to promote the mTOR activity. The downstream genes of mTOR also show a synchronized pattern to stimulate protein translation and lipid synthesis. The results demonstrate that cell cycle inhibition and stimulated mTOR activity at the transcriptome level are related to CHO cell size increase. The cell size increase is related to the extracellular nutrient conditions through a number of cascade pathways, indicating that by rational design of media and feeds, CHO cell size can be manipulated during culture processes, which may further improve cell growth and specific productivity.

1. Introduction

Chinese hamster ovary (CHO) cells are currently the predominant expression system for the production of biopharmaceuticals. In order to increase the volumetric productivity of CHO cell cultures, advances have been made with respect to media development, process optimization, and cell line engineering. To obtain an increased volumetric productivity without increasing cell density, an increase in specific productivity (q_p) is needed. For this, several strategies have been described, including hyperosmotic pressure,^[1] cell cycle arrest,^[2] and mild hypothermia.^[3] In these studies, the increase in q_p was found to be correlated with an increase in cell size. Furthermore, Kim et al.^[4] showed that the enhancement of the q_p was linearly correlated with an increase in cell size for nine CHO cell clones generated using the same transfection process. Edros et al.^[5] and Khoo and Al-Rubeai^[6] showed that the increase in q_p was directly related to the increase in cell volume due to enhancement of the transcription, translation, and secretion machinery.

The regulation of mammalian cell size is controlled by cell growth and cell division through multiple complex mechanisms and pathways.^[7,8] Proliferating cells are maintained at a more or less constant cell size by doubling their cell mass before each cell division. The mechanistic target of rapamycin (mTOR) signaling pathway has shown to be a central controller of cell size by controlling biomass synthesis.^[9–11] Dreesen and Fussenegger^[12] showed that an increase in the mTOR activity led to an increase in CHO cell size together with an up to fourfold higher protein content per cell, and a fourfold higher specific productivity of recombinant IgG. Furthermore, manipulation of the positive or negative upstream pathways of mTOR has been shown to influence mammalian cell size. Backman et al.^[13] showed that deletion of a mTOR inhibitor, phosphatase, and tensin homolog (PTEN), resulted in mammalian cell size increase. McVey et al.^[14] showed that the knock-out of another mTOR inhibitor, tuberous sclerosis complex 2 (TSC2), also resulted in larger CHO cells with higher protein synthesis and an over twofold increased q_p . In addition, an increase in the PI3K/Akt pathway activity which positively regulates mTOR resulted in cell size increase in both mammals and *Drosophila*.^[8]

Dr. X. Pan, A. A. Alsayyari, Prof. R. H. Wijffels, Dr. D. E. Martens
Bioprocess Engineering
Wageningen University and Research
PO Box 16, 6700 AA, Wageningen, The Netherlands
E-mail: dirk.martens@wur.nl

Dr. C. Dalm
Upstream Process Development
Synthon Biopharmaceuticals BV
PO Box 7071, 6503 GN, Nijmegen, The Netherlands

Dr. J. A. Hageman
Biometris
Wageningen University and Research
P.O. Box 16, 6700 AA, Wageningen, The Netherlands

Prof. R. H. Wijffels
Faculty of Biosciences and Aquaculture
Nord University
N-8049 Bodø, Norway

© 2018 The Authors. *Biotechnology Journal* Published by Wiley-VCH Verlag GmbH & Co. KGaA. This is an open access article under the terms of the Creative Commons Attribution License, which permits use, distribution and reproduction in any medium, provided the original work is properly cited.

DOI: 10.1002/biot.201800156

As mentioned before, cell size is also altered during the cycle of each cell division. Cell size and biomass content per cell increase during the interphase (G_1 , S, and G_2 phase) of the cell cycle. A cell reaches the largest cell size at the end of the G_2 phase, which is two times the size as the cell in the G_1 phase, before the mitosis (M phase) takes place.^[15] Hence, cell cycle control is also a way to increase cell size. In the study of Bi et al.,^[16] overexpression of the p21^{CIP1} induced G_1 -phase cell cycle arrest in a CHO cell culture, which resulted in nearly fourfold increase in cell volume as well as in q_p . In the study of Fomina-Yadlin et al.,^[17] the addition of small molecule inhibitors that arrest mammalian cells in the G_1 phase or G_1 /S transition resulted in a 1.5-fold increase in cell volume and q_p . The regulation of cell size is a complex process that involves a large network including both cell growth and division. Until now, the molecular mechanism of cell size regulation is not fully understood.

In our recent study,^[18] a cell number increase phase followed by a cell size increase phase was observed in a CHO cell fed-batch culture process using ActiCHO-P as basal medium and Actifeed A/B as feeds (from now on called the ActiCHO process). In the cell size increase phase, cell division comes to a halt but cell growth continues in the form of an increase in cell size. In this process, a standard feeding approach was used. No special strategies, such as lowering of the temperature, were used to arrest the cell cycle. The increase in cell volume was due to an increase in cell dry weight as a result of increases in protein, lipid, and carbohydrate content per cell. Furthermore, an increase in q_p was observed, which linearly correlated with the increase in cell volume. The metabolic changes associated with the cell size increase were studied in detail using flux balance analysis; however, the cause and molecular mechanisms for the cell size increase remained unclear. Transcriptome analysis has been used as a powerful tool to better understand the physiology of CHO cell lines.^[19–23] The aim of the present study is to obtain more insights into the cause and the molecular mechanisms underlying the CHO cell size increase using transcriptome analysis.

Due to the dynamic nature of the fed-batch culture (e.g., continuously changing cell density and nutrient and waste metabolite concentrations), many genes will be regulated over time of which only a part is related to the cell size increase. In order to enrich the genes that are related to cell size regulation, we used a FortiCHO process (FortiCHO basal medium fed with Efficient feed A/B) which did not result in cell size increase as a “filter.” The FortiCHO process is different in more aspects than only the cell size increase and consequently, not all genes that have a different expression profile between both processes will be related to the cell size increase. Nevertheless, many genes show an identical expression profile and are thus not uniquely related to the cell size increase.

2. Experimental Section

2.1. Cell Line and Fed-Batch Process Set-Up

A suspension CHO^{BC} cell clone (BC-P, provided by Bioceros Holding BV) producing a recombinant immunoglobulin G1 (IgG1) as previously described^[24] was used in this study. Two fed-batch processes using the same cell line but different

medium-feed systems are studied. One process resulted in cell size increase whereas for the other this was not the case.

- 1) *The ActiCHO culture process.* Triplicate fed-batch cultures were conducted in 10 L Sartorius bioreactors (sartorius stedim) controlled by BIOSTAT B-DCU II. Each bioreactor was inoculated with a starting density of 3×10^5 viable cells/mL at a starting volume of 5 L. Culture temperature was controlled at 37 °C, dissolved oxygen (DO) was controlled at 40% by pure O₂ flow enrichment, pH was controlled at 7.2 by CO₂ flow enrichment and 0.5 M NaOH. The feeding strategy was the same as described in Pan et al.^[18] Briefly, from day 3 on, 4.5% ActiCHO feed A and 0.45% ActiCHO feed B (both from GE Healthcare) per culture volume per day were fed to each reactor daily. 45% (w/w) glucose solution was added to each bioreactor, to ensure that the glucose concentration stayed above 5 mM at the next feeding point.
- 2) *The FortiCHO culture process.* Triplicate fed-batch cultures were conducted in 1 L DASGIP bioreactors (Eppendorf). Each bioreactor was inoculated with a starting density of 3×10^5 viable cells/mL at a starting volume of 500 mL. Culture temperature, DO, and pH are controlled at the same set-point as the ActiCHO process with similar approaches. From day 3 on, Efficient Feed A/B (with a 1:1 combination) was added to each bioreactor as one bolus. The feeding strategy was similar as described in Pan et al.^[24] Briefly, the daily volume added was calculated based on the specific glucose consumption rate, to ensure that the glucose concentration stayed above 5 mM at the next feeding point.

2.2. Daily Sampling and Analysis

A sample was taken from each bioreactor every day before the feed addition. Viable cell density (VCD), viability, and cell diameter were measured using a CedexHiRes analyzer (Innovatis; Roche) for the ActiCHO process, and a TC20 cell counter (Bio-Rad) for the FortiCHO process. Three milliliter of the sample was spun down at $300 \times g$ for 5 min (Heraeus Multifuge X3R, Thermo Scientific). The cell pellet was collected and the total RNA was extracted using 3 mL TRIzol reagent (Invitrogen) and stored at -80°C for later transcriptome analysis. For cell cycle analysis, 2 mL cell culture sample was spun down at $300 \times g$ for 5 min. The cell pellet was fixated in 2 mL ice-cold 70% ethanol overnight at -20°C . Next, the cells were prepared and stained using Cycletest Plus DNA Reagent Kit (BD Biosciences) and the cell cycle was analyzed on the BD Accuri C6 Flow Cytometer (BD Biosciences).

2.3. Transcriptome Analysis

For each bioreactor of the ActiCHO and FortiCHO process, transcriptome analysis was done for the samples taken on culture days 3, 5, and 7. Total RNA was purified using the RNeasy Mini kit (Qiagen, Valencia, CA). Affymetrix GeneChip CHO Gene 2.1 ST Arrays (Affymetrix, Santa Clara, USA) were used for transcriptome expression profiling. The detailed method was

presented in the study of Alsayyari et al.^[19] In short, the same amount of RNA was labeled by the Whole-transcript Sense Target Assay (Affymetrix) and hybridized according to the manufacturer's instructions. Quality control and data analysis were done as described in ref.^[25] Normalized expression estimates of probe sets were computed by the robust multi-array analysis (RMA),^[26] using R/Bioconductor package AffyPLM.^[27] The well-annotated reference sequences are based on the CriGri_1.0 genome assembly NCBI reference sequence project (RefSeq) Release 72, which resulted in 60626 annotated sequences (transcripts profiles) (custom CDF v20). After averaging the expression levels of probe sets targeting the same gene, expression data for 20858 unique genes were obtained, which was used for all subsequent analysis. Linear models (Limma package) were used to identify the differential expressed genes taking into account correlation due to the repeated sampling from the same bioreactors followed by an intensity-based moderated *t*-statistic.^[28,29] Gene regulations that satisfied the criterion of Benjamin and Hochberg false discovery rate (FDR.BH) <5% and absolute fold-change (FC) >1.4 were defined to be significant and were subjected to KEGG pathways over-representation analysis using Fisher's exact test. These cut-off values are applied to reduce the number of false-positive genes and the background noises that are picked up by the differential gene analysis.^[23,30–33]

3. Results and Discussion

3.1. Cell Growth, Cell Size, and Cell Cycle Dynamics

The cell growth characteristics including VCD, viability, and average cell diameter are shown in **Figure 1**. The VCD profile is similar for both processes (**Figure 1A**). The cell viability in the ActiCHO process (black-dashed line) started to decrease on day 10, while in the FortiCHO process (red dashed line) the decrease started on day 7. **Figure 1B** shows that for the ActiCHO process, upon the stop of cell division on day 5, the cells continued to grow in size, from an average cell diameter of 17 μm on day 4, to 24 μm on day 10. Our previous study on the ActiCHO process^[18] showed that the size increase was proportional to the increase in biomass content. In contrast, the average cell diameter in the FortiCHO process went down gradually from 17 μm on day 1, to 15 μm on day 7. The sharp decrease in cell diameter after day 7 was caused by cell death resulting in the formation of small particles which were probably apoptotic bodies. In addition, the monoclonal antibody product titre profiles of both processes are presented in **Figure S3**, Supporting Information.

To study the cell cycle status during the cell size increase of the ActiCHO process, the cell cycle distribution was measured. In **Figure 1C**, the propidium iodide (PI) DNA stain intensity area (FL2-A) which is a measure of the DNA content, is plotted against the forward scatter area (FSC-A) which is a measure of cell size for days 3, 5, 7, and 9. A clear cell cycle distribution can be seen at FL2-A intensities between 10 and 2 000 000. The populations observed above a FL2-A of 2 000 000 are probably due to aggregates. On day 3, they represent about 3% of the total events and they gradually disappear with the progression of culture time to about 1.5% on day 9. With culture time a

population develops at very low FL2-A intensities which probably represents cell debris and apoptotic bodies and agrees with the slight decrease in viability observed. It can be seen from **Figure 1C** that:

- 1) The cells in the G_2/M phase are larger (higher FSC-A) than the cells in the G_0/G_1 phase for all the analyzed culture days. This agrees with the fact that the volume and biomass per cell increase from the G_1 phase until the G_2/M phase.^[8]
- 2) Going from days 3 to 9, it can be seen that the S-phase population disappears and cells are arrested in both the G_0/G_1 and the G_2/M phase. When the cell debris population is gated out from the total population, the G_0/G_1 population presents 58% of the total population on day 3 and increases to 85% on day 9, whereas for the G_2/M population the number decreases from 31% on day 3 to 11% on day 9 (data not shown). The result agrees with the fact that after day 5 cell proliferation has stopped in the ActiCHO process (**Figure 1A**). In several CHO cell culture processes, hypothermia,^[34–36] hyperosmotic stress,^[1,37] and cell cycle inhibitors^[2,38,39] were applied that mediated a G_0/G_1 arrest without influencing G_2/M phase. This was, however, not the case in the present study where cell cycle arrest occurred in both G_0/G_1 and the G_2/M phase. In theory, cells at twice the FL2-A intensity could be aggregates of two cells arrested in the G_1 phase.
- 3) Cell size starts to increase after day 5 in both the G_0/G_1 and G_2/M phase, as shown by the increase in FSC-A values. The extent of the size increase in both phases is comparable. This indicates that the cell size increase is not influenced by the cell cycle phase the cell is arrested in. Rather, the cell biomass growth and cell cycle arrest seem to be two independent processes.

In summary, the cell cycle analysis confirms that the cell cycle arrest occurs in both the G_0/G_1 and the G_2/M phase of the ActiCHO process. Moreover, the cells arrested in both phases are able to grow in cell size.

3.2. Transcriptome Analysis

Transcriptome analysis using Affymetrix CHO Gene microarrays was performed to gain insights into the molecular mechanism underlying the cell cycle arrest and the cell size increase. The same amount of mRNA was brought on CHO Gene microarrays for each sample during the transcriptome analysis. Therefore, a change in gene expression is relative against the total transcripts and is not influenced by the possible fact that larger cells have a higher overall transcriptome activity.

The sample points on culture days 3, 5, and 7 of the two processes are selected for transcriptome analysis. Day 3 represents the middle of the cell proliferation phase where the cell size is still similar in both processes (**Figure 1A**). For the ActiCHO process, day 5 represents the start of the cell size increase phase whereas day 7 represents the middle of the cell size increase phase. For the FortiCHO process, day 5 represents the stop of exponential growth phase whereas day 7 represents the end of the stationary phase and the start of the death phase.

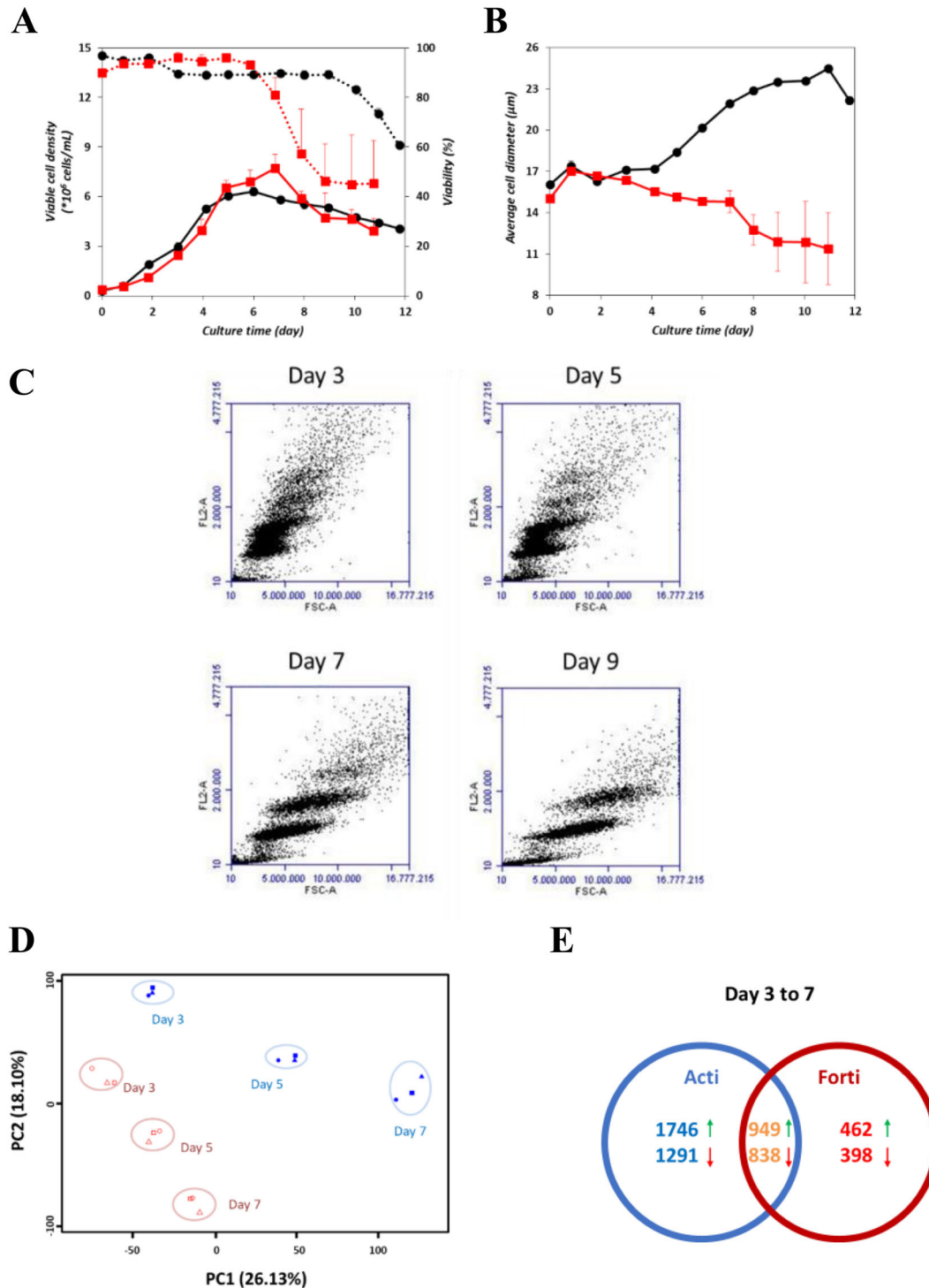


Figure 1. Cell growth, cell cycle, and transcriptome profiles of the fed-batch culture processes. A) VCD ($\times 10^6$ cells/mL, solid lines) and viability (%), and B) average cell diameter (μm) of the ActiCHO process published in Pan et al.^[18] (round mark, black lines) and the FortiCHO process (square mark, red lines). The error bars show the standard deviation for three bioreactors of each process. In A), only the positive error bars are shown in order to avoid overlap. C) The cell cycle analysis for the ActiCHO process on days 3, 5, 7, and 9. The propidium iodide (PI) DNA stain intensity (FL2-A) is plotted against the forward scatter area (FSC-A). FL2-A indicates the amount of DNA in a cell while FSC-A indicates the size of a cell. The sample events at high FL2-A intensity ($>2\,000\,000$) are likely caused by cell aggregates. D) Score plot generated from the transcriptome results of the ActiCHO (filled blue markers) and the FortiCHO (open red markers) processes. The same sample marker represents the sample taken from the same bioreactor. Samples taken from the same day and the same process is marked in a circle. Three biological replicates are included. E) Venn diagram of the number of genes that are differentially regulated from days 3 to 7 compared between the two processes. Upper numbers indicate up-regulation as shown by the green arrow, lower numbers indicate down-regulation as shown by the red arrow.

3.2.1. Transcriptome Profiles for Culture Processes With and Without a Cell Size Increase

The principal component analysis (PCA) (Figure 1D) shows the overall variation in gene expression for all analyzed samples. PC1 and PC2 contribute 26 and 18% to the total variation, respectively. The contribution for the rest of the PCs are minor (e.g., 7% of the PC3) and are not considered. PC1 and PC2 both capture a change in gene expression in time as well as a difference in gene expression between both systems (ActiCHO and FortiCHO). The Venn diagram (Figure 1E) shows the differential gene expression between days 3 and 7 which is unique to the ActiCHO and FortiCHO process, and which occurs in both processes. Genes are considered differentially expressed between the 2 days if the FDR.BH value is smaller than 5% and the absolute fold change is larger than 1.4 (see section 2.3). For the total 20 858 probed genes on the CHO gene array, 5684 genes (25%) are regulated in either the ActiCHO or FortiCHO process. In the ActiCHO process, 4824 genes (total number of genes in the blue circle) are differentially expressed, of which 3037 (total number of genes in the blue circle excluding the number of genes that overlap with the red circle) are unique to the ActiCHO process, and of which 1787 (overlap between the two circles) are also differentially expressed in the FortiCHO process in the same direction.

From the significantly regulated genes in the ActiCHO process from days 3 to 7, we first selected the top 10-fold-changes of the up- and down-regulated individuals (Table 1). Compared to the top 10-up- and down-regulated genes in the ActiCHO process, many of these genes also showed significant (fold-change >1.4, FDR.BH <5%) regulations in the FortiCHO process, however, the fold-changes are much smaller (see Supporting Information 1). In the top 10 up-regulated genes in the ActiCHO process, the *Fam213a* and *Ranbp3l* genes have extremely high fold-changes (188 and 145, respectively) compared to the others. The expression of *Fam213a* was shown to protect cells from oxidative stress.^[40] Oxidative stress in cells can be caused by increased reactive oxygen species (ROS) which are reduced forms of oxygen, such as superoxide radical (O_2^-), hydrogen peroxide (H_2O_2), and hydroxyl radical (HO^\cdot). The DO tension during all the cultures in this study was maintained at 40%. It is unlikely that a high extracellular DO was the cause of the ROS formation. However, increased oxidative metabolism was reported in CHO cells with increased mAb production as well as with increased cell size.^[16,41] In our previous study,^[18] a 1.5-fold increase in cellular oxygen consumption flux was observed during the size increase phase of the ActiCHO process. This might be related to the formation of ROS in cells and subsequently the overexpression of *Fam213a*. If this was the case, the extreme overexpression of *Fam213a* would likely be a response of the cell size increase, rather than the cause of it. Another extremely up-regulated gene, *Ranbp3l*, was reported to be involved in bone morphogenetic protein (BMP) signaling and regulating mesenchymal stem cell differentiation.^[42] The exact function of this gene in the context of cell size increase in CHO cells is however unknown. In addition, two genes involved in osmotic regulation (*Slc6a12* and *Scn7a*) are significantly up-regulated. This could be related to the increase in culture osmolality due to the feed addition which was described in our

Table 1. Top 10 fold-changes of up- and down-regulated genes in the ActiCHO process from days 3 to 7.

Gene symbol	Fold-change	Gene function in biological process
Top 10 up-regulation		
<i>Fam213a</i>	188.20	Redox regulation
<i>Ranbp3l</i>	145.63	Protein transport
<i>Sema4d</i>	24.12	Differentiation
<i>Spp1</i>	20.56	Cytokine activity, extracellular matrix binding
<i>Slc6a12</i>	19.64	Osmotic regulation/transport
<i>Myf9</i>	14.68	Myosin regulation
<i>Pcp4l1</i>	14.02	Protein coding
<i>Scn7a</i>	13.78	Sodium channeling
<i>S100a4</i>	11.42	Protein binding
<i>LOC100768899</i>	11.40	Protein coding
Top 10 down-regulation		
<i>Kif15</i>	-17.19	Mitosis, spindle assembly
<i>Ect2</i>	-16.84	DNA synthesis, cell cycle
<i>Nuf2</i>	-16.73	Mitosis, chromosome segregation
<i>Rrm2</i>	-16.55	DNA synthesis, cell cycle
<i>LOC100752904</i>	-15.90	nucleosome assembly
<i>Ccna2</i>	-14.97	Cell cycle
<i>Bub1b</i>	-14.87	Mitosis, chromosome segregation
<i>Cenpw</i>	-14.77	Mitosis, chromosome segregation
<i>Ccnb2</i>	-14.63	Cell cycle
<i>Aurkb</i>	-14.08	Mitosis, chromosome segregation

The gene functions are searched against the Gene Ontology (GO) and UniProt database. The results generated are based on three bioreactor cultures.

previous study for the ActiCHO process.^[18] Next to the top 10 up-regulated genes, also the top 10 down-regulated genes are listed in Table 1, together with the functions of these genes in biological processes. As can be seen, all the top 10 down-regulated genes are involved in cell cycle regulation and mitosis. This agrees with the inhibition of cell cycle progression as described in the previous section. Some of these genes are further discussed in the next section.

In order to get a better understanding of the relationship between gene regulation and the cell size increase, a targeted approach is used in the next sections. From the genes that are differentially expressed in the ActiCHO process (the blue circle in Figure 1E), a subset of genes (≈ 500 genes in total) are examined in more detail. This subset of genes are selected based on the fact that they are known to play critical roles in cell cycle progression and biomass growth as well as in the signaling pathways involved in these processes. The regulation of these genes is compared to that in the FortiCHO process, to enrich genes that are uniquely related to the cell size increase. An overview of the selected pathways is shown in Figure 2. Note that some pathways in Figure 2 are known to be post-transcriptional regulated (e.g., by phosphorylation), and it is not completely clear whether they are regulated transcriptionally as well. Thus, genes that are not differentially expressed could still be

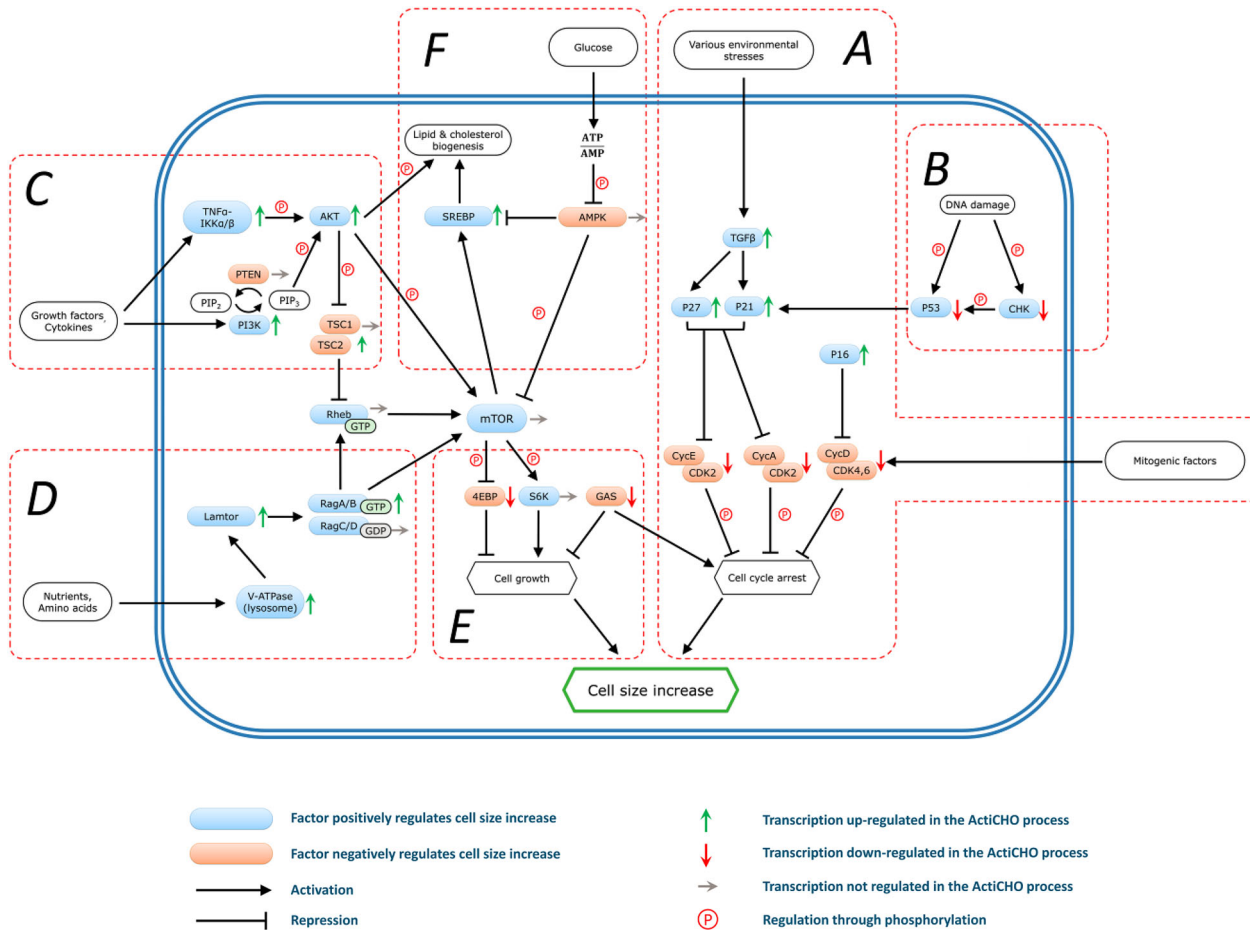


Figure 2. Overview of the signaling pathways regulating cell cycle arrest and the cell size increase. CDK, cyclin dependent kinases; Cycs, cyclins; TGFβ, transforming growth factor beta; CHK, checkpoint kinases; p53, tumor protein p53; p16, p21, and p27, cyclin-dependent kinase inhibitors, p16^{INK4a}, p21^{CIP1}, and p27^{KIP1}, respectively; TNFα-IKKα/β, tumor necrosis factor-α (TNFα)—inhibitor of nuclear factor-κB kinase-β (IKKβ); AKT, Protein Kinase B; TSC1/2, tuberous sclerosis complex 1/2; PTEN, phosphatase and tensin homolog; PI3K, phosphatidylinositol 3'-kinase; Rheb, Ras homolog enriched in brain; mTOR, mechanistic target of rapamycin; V-ATPase, vacuolar H⁺-ATPase; AMPK, AMP-activated protein kinase; GAS, growth arrest specific; SREBP, sterol responsive element binding; 4EBP, eukaryotic translation initiation factor 4E binding protein; Lamtor, late endosomal/lysosomal adaptor; S6K, P70-S6 Kinase 1; RagA/B and RagC/D, Rag heterodimers A/B and C/D.

important due to post-transcriptional regulation. However, if the transcription of these pathways shows a synchronized regulation, it may still mean that at least part of the regulation is done transcriptionally, and it may still give an indication of these gene functions in cell size increase.

3.2.2. Gene Regulation Related to Cell Cycle Arrest

Figure 2A,B shows the pathways related to the cell cycle regulation. The genes of these pathways that are significantly regulated from culture days 3 to 7 in the ActiCHO process are presented and their changes in expression are compared to those in the FortiCHO process (Table 2). Mammalian cell cycle regulation involves the participation of two classes of proteins: the cyclin-dependent kinases (Cdks), and their binding partners, cyclins (Cycs).^[43] Binding of a Cdk to a Cyc forms an active complex that enables the cell cycle to progress through a specific phase. For both processes in

Table 2, down-regulations of various cdk genes and their binding partner cyclin genes (*Cycs*) are observed, which agrees with the stop of cell division in both processes. However, the extent of down-regulation (fold change) and significance (FDR. BH) for these genes are much higher in the ActiCHO process than in the FortiCHO process, indicating that the cell cycle arrest is stronger in the ActiCHO process.

For the ActiCHO process, especially one *CycA* gene (*Ccna2*, FC = -14.97, FDR.BH < 0.5%), two *CycB* genes (*Ccnb1*, FC = -11.20, FDR.BH < 0.5%, and *Ccnb2*, FC = -14.63, FDR.BH < 0.5%), and to a lesser extent a *Cdk* gene (*Cdk1*, FC = -3.89, FDR.BH < 0.5%), have much stronger down-regulations as compared to the other Cdk and Cyc genes (Table 2). Binding of *CycA* with *Cdk1* is required for the G₂/M transition,^[15] binding of *CycA* with *Cdk2* plays an important role in S phase progression and DNA replication,^[44] and binding of *CycB* with *Cdk1* is required for mitosis.^[15] The strong down-regulation of *CycA*, *CycB*, and *Cdk1* genes in the ActiCHO process agrees with the observed arrest of the cell cycle in G₂/M phase and indicates a

Table 2. Fold change (FC) cell cycle related genes from culture days 3 to 7 in the culture with cell size increase (ActiCHO) and with no cell size increase (FortiCHO).

	FC. ActiCHO	FDR.BH	FC. FortiCHO	FDR.BH
Cyclin-dependent kinase (Cdk) (promote)				
<i>Cdk1</i>	-3.89	<0.5%	-1.17	9%
<i>Cdk2</i>	-2.29	<0.5%	-1.76	<0.5%
<i>Cdk4</i>	-2.19	<0.5%	-1.36	<0.5%
<i>Cdk5</i>	1.47	<0.5%	-1.03	81%
<i>Cdk6</i>	-1.74	<0.5%	-1.02	79%
<i>Cdk15</i>	1.55	1%	2.21	<0.5%
Cyclin (Cyc) (promote)				
<i>Ccna2</i>	-14.97	<0.5%	-1.77	<0.5%
<i>Ccnb2</i>	-14.63	<0.5%	-1.60	<0.5%
<i>Ccnb1</i>	-11.20	<0.5%	-1.64	<0.5%
<i>Ccne2</i>	-3.09	<0.5%	-1.85	<0.5%
<i>Ccnf</i>	-2.63	<0.5%	-1.68	<0.5%
<i>Ccne1</i>	-2.31	<0.5%	-2.58	<0.5%
<i>Ccng1</i>	1.41	<0.5%	-1.22	3%
<i>Ccng2</i>	2.34	<0.5%	1.70	<0.5%
Cyclin-dependent kinase inhibitor (CDKN) (arrest)				
<i>Cdkn2a</i>	1.62	<0.5%	1.11	24%
<i>Cdkn1a</i>	1.73	<0.5%	1.28	<0.5%
Transforming growth factor beta (TGFβ) (arrest)				
<i>Tgfb3</i>	2.13	<0.5%	1.02	93%
<i>Tgfb2</i>	1.61	<0.5%	1.15	1%
Checkpoint kinase (CHEK) (arrest)				
<i>Chek1</i>	-2.80	<0.5%	-1.37	<0.5%
<i>Chek2</i>	-2.47	<0.5%	-1.23	6%
Tumor protein p53 (P53) (arrest)				
<i>Tp53</i>	-1.77	<0.5%	-1.79	<0.5%

Positive values mean up-regulation and negative values mean down-regulation. Genes with a FDR.BH < 5% and the absolute FC > 1.4 are considered significant and are shown here. (Arrest) means the genes promote cell cycle arrest whereas (promote) means the genes promote cell cycle progression. The results generated are based on three bioreactor cultures for both the ActiCHO and the FortiCHO process.

delay in S phase and mitosis. In addition, binding CycE with Cdk2 is required for progression through the G₁/S phase.^[45] The down-regulation of *Cdk2* (FC = -2.29, FDR.BH < 0.5%) may be related to the cell cycle arrest in the G₁ phase.

In order to find the cause of the cell cycle arrest, next, signaling pathways that coordinate the cell cycle are studied. The cell cycle activities are regulated by a number of Cdk inhibitors (Cdkns) such as p16^{INK4a} (*Cdkn2a*), p21^{CIP1} (*Cdkn1a*), and p27^{KIP1} (*Cdkn1b*)^[15] (Figure 2A). Binding of these Cdkns to the Cdkns inhibits formation of the active Cdk/Cyc complexes, which suppresses the cell cycle progression.^[43] The high up-regulations of *Cdkns* (*Cdkn2a*, FC = 1.62, FDR.BH < 0.5%, and *Cdkn1a*, FC = 1.73, FDR.BH < 0.5%) in the ActiCHO process indicate a strong cell cycle inhibition (Table 2). In contrast, the *Cdkns* in the FortiCHO process showed much less regulation (*Cdkn2a*,

FC = 1.11, FDR.BH = 24%, and *Cdkn1a*, FC = 1.28, FDR.BH < 0.5%).

Cell cycle inhibitors can be activated by intracellular stimuli (e.g., DNA damage), or extracellular stimuli (e.g., deprivation of mitogenic factors).^[46] The regulation pathways related to intracellular DNA damage are shown in Figure 2B. Upon sensing DNA damage, checkpoint kinases (encoded by *Chek1* and *Chek2*), and the p53 tumor suppressor protein (encoded by *Tp53*) can be phosphorylated and activated, resulting in the G₁ and G₂ cell cycle inhibition.^[47] Although these steps are regulated via post-transcriptional phosphorylation, the significant down-regulations of *Chek1*, *Chek2*, and *Tp53* genes in both of the two processes (Table 2) imply that DNA damage is less likely the cause of the cell cycle arrest. With regard to extracellular stimuli, the p21^{CIP1} can be induced by transforming growth factor beta (TGFβ, encoded by *Tgfb*), which acts as a negative paracrine/autocrine growth factor in growth regulation,^[48–50] as shown in Figure 2A. The TGFβ protein is activated from its latent complex upon sensing various environmental stresses such as ROS,^[51] hypoxic conditions,^[52] pH,^[53] and proteases.^[54] As mentioned before, the DO and pH are well controlled during both the ActiCHO and the FortiCHO processes. Furthermore, at the point where cell size started to increase in the ActiCHO process (culture day 4, Figure 1A), the biomass concentration of both process are comparable, therefore, ROS and hypoxia are not likely the cause of different TGFβ activities in both processes and through that play a role in cell size increase. The TGFβ signaling pathway is initiated by binding of TGFβ to TGFβ receptors (types I and II encoded by *Tgfb1* and *Tgfb2*) and subsequently, induces p27^{KIP1} and p21^{CIP1} leading to the cell cycle inhibition (Figure 2A). The higher up-regulations of both the *Tgfb* (*Tgfb3*, FC = 2.13, FDR.BH < 0.5%) and *Tgfb* (*Tgfb2*, FC = 1.61, FDR.BH < 0.5%) genes in the ActiCHO process (Table 2) indicate a higher TGFβ signaling activity. In addition, expression of CycD is strongly dependent on extracellular mitogens. The CycD/CDK4, 6 complexes, therefore, function early in G₁ and act as mitogen sensors (Figure 2A).^[55] The CycD genes (*ccnd1*, *ccnd2*, and *ccnd3*) are not regulated in the ActiCHO process (Supporting Information 1), indicating that deprivation of extracellular mitogens is not likely the cause of cell cycle arrest in the G₁ phase. However, looking at the expression of various mitogen-activated protein kinases (Supporting Information 1), we find both significant up- and down-regulations in the ActiCHO process. Therefore, it is not certain whether lacking of mitogen is the cause of the cell cycle arrest in the phases other than G₁. In summary, the result from transcriptome analysis implies that the cell cycle arrest in the ActiCHO process was caused by an activation of cell cycle inhibitors and down-regulation of Cdkns and cyclins in reaction to extracellular environmental stresses and/or depletion of mitogen(s).

3.2.3. Gene Regulation Related to Cell Growth

Besides the cell cycle arrest, a continued biomass production is the other essential aspect for cell size increase. In this context, we found that in agreement with literature, the mTOR pathway is playing a central role in manipulating the cell biomass growth of

the ActiCHO process. mTOR integrates the extracellular and intracellular signals through a number of upstream pathways, and regulates cell growth through its downstream effectors.^[56] The regulation of these pathways in the ActiCHO process are summarized in Figure 2C–F. In addition, the significantly regulated genes involved in these pathways are shown in Table 2.

First of all, the downstream effectors of mTOR are studied. The activity of these effectors are regulated by mTOR in transcriptional and/or post-transcriptional approaches. Activation of mTOR results in phosphorylation of the eukaryotic initiation factor 4E-binding proteins (4EBPs). The phosphorylation prevents binding of these proteins to the eukaryotic initiation factor eIF4E.^[10] This results in increased activity of eIF4E, which promotes protein translation.^[57] In the ActiCHO process, the eukaryotic initiation factor 4E-binding protein (4EBP) genes are significantly down-regulated (*Eif4ebp1*, FC = -2.53, FDR.BH < 0.5% and *Eif4ebp2*, FC = -1.40, FDR.BH < 0.5%). The down-regulation of 4EBP genes may have resulted in less binding to eIF4E and thus, released the activity of protein synthesis (see Figure 2E). As a result, the protein synthesis rate in the ActiCHO process remained high during the size increase phase. In contrast, the 4EBP genes are not regulated (*Eif4ebp1*, FC = -1.06, FDR.BH = 67% and *Eif4ebp2*, FC = -1.09, FDR.BH = 40%) in the FortiCHO process, which agrees with the stopped cell growth in this process.

High mTOR activity also positively regulates the synthesis of lipids^[58] which is a necessary component for cell growth (see Figure 2F). An increase in mTOR complex 1 (mTORC1) activity was reported to increase the sterol responsive element binding protein (SREBP) activity which led to higher lipid synthesis rate.^[59] The higher up-regulation of the SREBP gene (*Srebf1*, FC = 1.47, FDR.BH = 3%) in the ActiCHO process correlates with the slightly higher fatty acid synthesis rate during the cell size increase phase compared to the proliferation phase and the formation of lipid droplets, as shown in our previous study.^[18] In contrast, the SREBP gene is not regulated (FC = -1.02, FDR.BH = 94%) in the FortiCHO process. In addition to by mTOR, lipid synthesis was also shown to be induced by Akt which is a positive upstream regulator of mTOR. Akt induces lipid synthesis by up-regulating the ATP citrate lyase (encoded by *Acly* gene) activity. ATP citrate lyase is a key enzyme that catalyzes the reaction from citrate to cytosolic oxaloacetate and acetyl-CoA.^[60] The latter one is a precursor for lipogenesis. In the ActiCHO process, the transcriptional activity of the *Acly* gene remained unchanged (FC = -1.03, FDR.BH = 72%, see Supporting Information 1) whereas in the FortiCHO process, it decreased significantly (FC = -1.87, FDR.BH < 0.5%, see Supporting Information 1). In agreement with the transcriptome data, the fatty acids synthesis rate in the ActiCHO process was maintained more or less constant during the cell size increase phase as compared to the exponential growth phase. In contrast, the pathways related to lipid synthesis experienced significant down-regulations in the FortiCHO process, which agrees with the fact that the cells went from the exponential growth phase on day 3 to the stationary phase on day 7 since the requirement for lipids went down.

Next, cascade pathways upstream of mTOR that channel extracellular signals to mTOR were studied (Figure 2C,D,F). The differentially expressed genes in these pathways are shown in

Table 3. The presence of extracellular growth factors and nutrients are essential to the growth and biomass synthesis of the cells. A lack of either growth factors or nutrients can lead to growth attenuation, autophagy, and eventually cell death.^[61] The concentration of extracellular growth factors and nutrients is sensed by the cells through a number of signaling pathways. The signal of growth factors, such as insulin-like growth factors (IGF), is channeled through the PI3K-Akt pathway.^[62] The signal transduction starts with the binding of IGF to the IGF binding protein (IGFBP, encoded by *Igfbps* genes).^[63] Next, the binding of IGF with IGFBP phosphorylates phosphatidylinositol (4,5) biphosphate (PIP2) to produce PIP3 (Figure 2C).^[64] The later one phosphorylates and activates the Akt pathway which subsequently promotes the mTOR activity, as mentioned previously. In the ActiCHO process, *Igfbps* showed stronger up-regulations (*Igfbps7*, FC = 1.90, FDR.BH < 0.5%, and *Igfbps4*, FC = 1.51, FDR.BH < 0.5%) compared to in the FortiCHO process (*Igfbps7*, FC = 1.15, FDR.BH = 57%, and *Igfbps4*, FC = -1.34, FDR.BH < 0.5%) (Table 3). In agreement with this, it also can be seen in Table 3 that the PI3K (*Pik3ip1* and *Pik3c2a*) genes are significantly up-regulated in the ActiCHO process.

Besides the PI3K pathway, increasing evidence suggests that cytokines, such as tumor necrosis factor- α (TNF α) through the inhibitor of nuclear factor- κ B kinase- β (IKK β) mediated pathway, can also induce the Akt activity.^[65] It can be seen in Table 3 that various genes for the TNF α -induced proteins (*Tnfaiip*) are up-regulated much stronger in the ActiCHO process compared to in the FortiCHO process. Both the PI3K and the TNF α -IKK β pathways have a similar expression pattern in the ActiCHO process, and both have a positive contribution to the Akt activity. This together demonstrates that the extracellular growth factors and cytokines are likely the important factors for the activation of the Akt and subsequently the mTOR activity, meaning that they are also likely the cause of the cell size increase after the cell cycle inhibition.

In addition to the growth factors and cytokines, sufficient extracellular amino acids concentrations are needed to maintain the mammalian cell growth. The signaling pathways related to sensing the amino acid levels are illustrated in Figure 2D. Sufficient amino acid levels stimulate the vacuolar H⁺-ATPase (v-ATPase) on the lysosomal membrane,^[66] leading to hydrolysis of ATP by v-ATPase. This signal stimulates the regulator complex (encoded by the late endosomal/lysosomal adaptor, *Lamtor* genes) activity. The regulator complex acts as a guanine exchange factor converting Raga/B · GDP to Raga/B · GTP.^[66] The latter one can bind to and activate the mTORC1. As can be seen in Table 3, several V-ATPase and *Lamtor* genes show higher up-regulation in the ActiCHO process compared to in the FortiCHO process, implying that the signals from the amino acids sensing pathways also play a role in promoting the mTOR activity for the continued biomass growth in the ActiCHO process. As can be seen in Figure S5, Supporting Information, amino acid concentrations in the FortiCHO process are substantially different from those in the ActiCHO process, which may have caused the differences in growth behavior, although it cannot be excluded that other factors in the complex media are involved. The higher concentrations of amino acids in the ActiCHO process does correlate with the higher activity of the amino acid sensing pathways in this

Table 3. Fold change (FC) mTOR upstream and downstream genes from culture days 3 to 7 in the culture with cell size increase (ActiCHO) and with no cell size increase (FortiCHO).

	FC. ActiCHO	FDR.BH	FC. FortiCHO	FDR.BH
mTOR downstream effectors				
Eukaryotic translation initiation factor 4E-binding protein (4EBP) (inhibit)				
<i>Eif4ebp1</i>	-2.53	<0.5%	-1.06	67%
<i>Eif4ebp2</i>	-1.40	<0.5%	-1.09	40%
Sterol regulatory element-binding protein (SREBP) (promote)				
<i>Srebf1</i>	1.47	3%	-1.02	94%
mTOR upstream regulators				
Insulin-Like Growth Factor-binding protein (IGFBP) (promote)				
<i>Igfbp7</i>	1.90	<0.5%	1.15	57%
<i>Igfbp4</i>	1.51	<0.5%	-1.34	<0.5%
TNF alpha induced protein (TNFaIP) (promote)				
<i>Tnfaip6</i>	4.21	<0.5%	1.55	1%
<i>Tnfaip2</i>	3.32	<0.5%	1.05	84%
<i>Tnfaip8</i>	1.69	<0.5%	-1.22	20%
<i>Tnfaip1</i>	1.41	<0.5%	-1.06	64%
<i>Tnfaip3</i>	-1.43	<0.5%	-1.30	2%
Phosphoinositide 3-kinase (PI3K) (promote)				
<i>Pik3ip1</i>	2.01	<0.5%	1.47	3%
<i>Pik3c2a</i>	1.76	<0.5%	1.01	94%
Protein kinase B (PKB/AKT) (promote)				
<i>Akt2</i>	1.40	<0.5%	1.12	4%
Tuberous sclerosis complex (TSC) (inhibit)				
<i>Tsc2</i>	1.45	<0.5%	1.11	18%
Vacuolar-type H ⁺ -ATPase (V-ATPase) (promote)				
<i>Atp6v1f</i>	1.64	<0.5%	1.23	5%
<i>Atp6v1a</i>	1.62	<0.5%	1.26	<0.5%
<i>Atp6v1b2</i>	1.54	<0.5%	1.45	<0.5%
<i>Atp6v1e1</i>	1.43	<0.5%	1.16	3%
Late endosomal/lysosomal adaptor, MAPK and MTOR activator (Lamtor) (promote)				
<i>Lamtor2</i>	1.51	<0.5%	1.08	58%
<i>Lamtor4</i>	1.22	4%	1.23	7%
<i>Lamtor5</i>	1.2	3%	-1.01	93%
AMP-activated protein kinase (AMPK) (inhibit)				
<i>Prkaa1</i>	1.42	<0.5%	1.08	32%
Growth arrest specific (GAS) (inhibit)				
<i>Gas2</i>	-5.77	<0.5%	-1.95	<0.5%
<i>Gas2l3</i>	-5.66	<0.5%	-1.18	11%
<i>Gas7</i>	-1.78	<0.5%	-1.30	13%

Positive values mean up-regulation and negative values mean down-regulation. Genes with a FDR.BH < 5% and the absolute FC > 1.4 are considered significant and shown here. (Promote) means the genes promote biomass synthesis whereas (inhibit) means the genes hamper biomass synthesis. The results generated are based on three bioreactor cultures for both the ActiCHO and the FortiCHO process.

medium, as can be seen in section in Table 3 on the regulation of the V-ATPase and *Lamtor* genes.

Glucose is a major nutrient for CHO cell lines. The characteristic consumption rate of glucose and the concomitant production rate of lactate are typically high in CHO cell lines. In addition, as shown in our previous study,^[24] the specific glucose consumption rate during the size increase phase of the ActiCHO process is significantly higher than it is during the stationary phase of the FortiCHO process, which can also be seen in Figure S4, Supporting Information. The high glucose consumption is likely the result of a high glycolysis activity and will correspondingly result in a high intracellular ATP/AMP ratio. The high ATP/AMP ratio can suppress the AMP-activated protein kinase (AMPK) activity^[67] and lead to an increased mTOR activity through phosphorylation (Figure 2F). In this study, we are unable to confirm the state of the ATP/AMP ratio. However, one AMPK transcript (*Prkaa1*) showed an up-regulation in the ActiCHO process (Table 3). Assuming the AMPK pathway is also regulated transcriptionally, this implies a decrease in the ATP/AMP ratio. In this regard, the high specific glucose consumption rate (Figure S4, Supporting Information) seems to play no role in activating mTOR during the cell size increase of the ActiCHO process.

Furthermore, several growth arrest specific (*Gas*) genes showed high (>5 FC) down-regulations in the ActiCHO process (Table 3). Expression of the Gas protein family is strictly related to the growth arrest state of mammalian cells^[68,69] (see Figure 2E) and may be involved in various cellular activities including microfilaments reorganization, cell cycle, DNA synthesis, and apoptosis.^[68,70,71] Smith and Steitz^[72] showed that upon reduction of the mTOR activity, *Gas5* transcript levels increased. Recently, the *Gas5* transcript was shown to be an important tumor suppressor involved in various cancers.^[73] In addition, the expression of *Gas2* transcript has been shown to play a critical role in preventing cancer transformation by leading the cells to a premature senescence.^[74] In the present work, greater down-regulations of the *Gas* genes in the ActiCHO process correlates with the continued cell growth in the ActiCHO process. It is, however, not fully clear how these *Gas* genes interact with intra- and extracellular signals to participate in growth control.

Summarizing this section, it was shown that the mTOR upstream and downstream pathways were regulated in a strongly synchronized pattern in the ActiCHO process, leading to a higher mTOR activity in this process. In the FortiCHO process, this was not observed. These results demonstrate that the activation of mTOR plays an essential role in the continued biomass growth after the stop of cell cycle progression. Furthermore, the activation of mTOR is closely related to the extracellular growth factors, cytokines, and amino acids levels, indicating that the cell size increase is related to these extracellular conditions.

3.3. Extracellular Stimuli for the Cell Size Increase

The cell size increase in this study is associated with the cell cycle arrest and the continued biomass formation. Two genes involved in osmotic regulation (*Slc6a12* and *Scn7a*) showed up in the top 10 up-regulated fold changes (Table 1). However, in a perfusion

process using the same cell line and the ActiCHO-P medium as perfusion medium, a comparable change in cell size was observed (data not shown). In that experiment, the ActiCHO feed A/B was not used and the culture osmolality was constant. It can therefore be concluded that the cell cycle arrest and the concomitant cell size increase are not related to the osmolality nor to a unique feature of the ActiCHO feed A/B.

A significant cell cycle arrest was observed in the ActiCHO process. Cell cycle arrest could be caused by secretion of toxic metabolites (e.g., ammonium and lactate) or paracrine/autocrine proteins (e.g., TGF β). Cell division stopped and cell size started to increase on day 4. At this time the lactate and ammonium concentrations were about 25 and 3 mM, respectively. Based on a survey on all our experiments done in controlled bioreactors with the same cell line in different media systems (unpublished), the cells can still divide rapidly at lactate and ammonium concentrations of 40 and 5 mM, respectively. Thus, ammonium and lactate are not likely the cause of the cell cycle arrest. The TGF β pathway is significantly up-regulated in the ActiCHO process, which may have caused cell cycle arrest. Another cause of the cell cycle arrest could be depletion of certain nutrients or mitogenic factors. If this was the case, these nutrients or mitogenic factors should not be present in the feeds or that the depletion causes irreversible cell cycle arrest which cannot be released by addition of the depleted nutrients anymore. This means that these factors are absent or not present in sufficient amounts in the feed. It could also be that depletion of a nutrient in the batch period causes the cells to enter a non-proliferative state from which it cannot recover by later addition of that nutrient. For example, in Figure S5, Supporting Information, it can be seen that in the ActiCHO process some non-essential amino acids including asparagine, glutamine, and cystine were depleted around the point where cells stopped dividing and started increasing size (day 5). Fomina-Yadlin et al.^[75] reported that depletion of individual amino acid can activate the amino acid response pathway (AAR), resulting in an overexpression of activating transcription factor 4 (ATF4). Consequently, cells experience down-regulation of cell cycle progression, DNA replication, nucleotide biosynthesis, and lipid metabolism. However, in the present study, the ATF4 gene (ATF4) was significantly down-regulated from days 3 to 7 (FC = -4.2, FDR.BH < 0.5%, Supporting Information 1), indicating that the AAR pathway was not triggered on day 7. Since depletion occurred at day 3 and was resolved by feed addition at day 7, it could still be that a temporary overexpression between days 3 and 7 of ATF4 triggered the AAR pathway at the moment of depletion of certain amino acid(s) and caused an irreversible cell cycle arrest. In the meantime, the high concentration of the other amino acids (see Figure S5, Supporting Information) keeps the mTOR activity high resulting in continued biomass production and cell size increase. Note that in the FortiCHO process, the same non-essential amino acids asparagine, glutamine, and cystine were also depleted around day 5. However, the other amino acids levels are significantly lower compared to in the ActiCHO process, which may be related to the lower mTOR activity in the FortiCHO process. This hypothesis, however, needs to be further confirmed by a higher time resolution for the transcriptome data and by tuning the amino acids ratio in the ActiCHO process.

Since cell size increase is positively correlated to the increase in cell specific recombinant protein productivity, it would be beneficial to design the medium and feed system in a way to trigger the cell size increase in a fed-batch culture process through, for example, inducing the mTOR activity. On the other hand, since biomass continues to grow after the stop of cell division in such a process, the nutrients provided to the culture should contain not only nutrients assigned for maintenance and mAb production reactions, but also all the precursors and building blocks for biomass growth.^[18]

4. Conclusion

We performed a transcriptome analysis to identify the molecular mechanism associated with cell size increase for a CHO fed-batch process. Looking at the top 10-fold changes of up- and down-regulated genes in the ActiCHO process, genes related to redox regulation, protein transport, and osmotic regulations were highly up-regulated. This result indicates that cells adapted transcriptionally to cope with redox and osmotic changes during the culture process. In addition, the top 10 down-regulated genes were related to cell cycle regulation and mitosis. This agrees with the observed cell size increase and cell cycle arrest in the ActiCHO process. In the next step, genes involved in cell cycle progression and biomass growth as well as in the signaling pathways of these processes were selected for further analysis. It was found that various cyclin (*cyc*) and *cdk* genes were significantly down-regulated in the ActiCHO process, and a number of Cdk inhibitors (Cdkns) were significantly up-regulated, which agrees with the cell cycle arrest in both the G₀/G₁ and the G₂/M phase. The gene expression results also indicate that the cell cycle arrest is not caused by DNA damage. Looking at the genes involved in regulation of biomass growth, the mTOR upstream and downstream pathways are regulated in a strongly synchronized pattern to stimulate the mTOR activity in the ActiCHO process. This agrees with a continued cell growth after cell cycle arrest. It is possible that the production of TGF β as a negative paracrine/autocrine factor, or the depletion of certain nutrients and/or mitogenic factors in the basal medium resulted in the cell cycle arrest. Meanwhile, extracellular growth factors and high nutrients levels keep channeling the mTOR activity to maintain biomass production. This study showed that the continued biomass growth after the cell cycle arrest is related to the extracellular nutrient levels. Hence, by rational design of media and feeds, it may be possible to manipulate CHO cell size during industrial culture processes, which will further improve cell growth and specific productivity.

Supporting Information

Supporting Information is available from the Wiley Online Library or from the author.

Acknowledgements

This research project was financially supported by the EFRO Province of Gelderland and Overijssel, the Netherlands. The authors thank Bioceros

Holding BV, for providing the CHO^{BC} clone, and the upstream process development department of Synthron Biopharmaceuticals BV for supporting the 10L culture experiments. The authors also thank Jianan Wang for helping with the cell cycle analysis.

Conflict of Interest

The authors declare no commercial or financial conflict of interest.

Keywords

cell cycle, cell size increase, CHO cell culture, mAb production, mTOR, transcriptome analysis

Received: March 21, 2018
Revised: July 11, 2018
Published online: July 30, 2018

- [1] Z. Sun, R. Zhou, S. Liang, K. M. McNeeley, S. T. Sharfstein, *Biotechnol. Prog.* **2004**, *20*, 576.
- [2] A. V. Carvalhal, I. Marcelino, M. J. T. Carrondo, *Appl. Microbiol. Biotechnol.* **2003**, *63*, 164.
- [3] V. S. Martínez, M. Buchsteiner, P. Gray, L. K. Nielsen, L.-E. Quek, *Metab. Eng. Commun.* **2015**, *2*, 46.
- [4] T. K. Kim, J. Y. Chung, Y. H. Sung, G. M. Lee, *Biotechnol. Bioprocess Eng.* **2001**, *6*, 332.
- [5] R. Edros, S. McDonnell, M. Al-Rubeai, *BMC Biotechnol.* **2014**, *14*, 15.
- [6] S. H. G. Khoo, M. Al-Rubeai, *Biotechnol. Bioeng.* **2009**, *102*, 188.
- [7] I. Conlon, M. Raff, *Cell* **1999**, *96*, 235.
- [8] P. Jorgensen, M. Tyers, *Curr. Biol.* **2004**, *14*, 1014.
- [9] J. J. Howell, B. D. Manning, *Trends Endocrinol Metab.* **2011**, *22*, 94.
- [10] M. Laplante, D. M. Sabatini, *J. Cell Sci.* **2009**, *122*, 3589.
- [11] P. B. Dennis, a Jaeschke, M. Saitoh, B. Fowler, S. C. Kozma, G. Thomas, *Science* **2001**, *294*, 1102.
- [12] I. A. J. Dreesen, M. Fussenegger, *Biotechnol. Bioeng.* **2011**, *108*, 853.
- [13] S. A. Backman, V. Stambolic, A. Suzuki, J. Haight, A. Elia, J. Pretorius, M. S. Tsao, P. Shannon, B. Bolon, G. O. Ivy, T. W. Mak, *Nat. Genet.* **2001**, *29*, 396.
- [14] D. McVey, M. Aronov, G. Rizzi, A. Cowan, C. Scott, J. Megill, R. Russell, B. Tirosh, *Biotechnol. Bioeng.* **2016**, *113*, 1942.
- [15] K. Vermeulen, B. Van Bockstaele, K. Vermeulen, D. R. Van Bockstaele, Z. N. Berneman, *Cell Prolif.* **2003**, *36*, 131.
- [16] J. X. Bi, J. Shuttlesworth, M. Al-Rubeai, *Biotechnol. Bioeng.* **2004**, *85*, 741.
- [17] D. Fomina-Yadlin, Z. Du, J. T. McGrew, *J. Biotechnol.* **2014**, *189*, 58.
- [18] X. Pan, C. Dalm, R. H. Wijffels, D. E. Martens, *Appl. Microbiol. Biotechnol.* **2017**, *101*, 8101.
- [19] A. A. Alsayyari, X. Pan, C. Dalm, J. W. van der Veen, N. Vriezen, J. A. Hageman, R. H. Wijffels, D. E. Martens, *J. Biotechnol.* **2018**, *279*, 61.
- [20] A. J. Brown, S. Gibson, D. Hatton, D. C. James, *Biotechnol. J.* **2018**, *13*, 1.
- [21] A. Singh, H. F. Kildegaard, M. R. Andersen, *Biotechnol. J.* **2018**, *1800070*, 1800070.
- [22] D. Vito, C. M. Smales, *Biotechnol. J.* **2018**, 1800122. <https://doi.org/10.1002/biot.201800122>
- [23] C. Chen, H. Le, B. Follstad, C. T. Goudar, *Biotechnol. J.* **2018**, *13*, 1800122.
- [24] X. Pan, M. Streefland, C. Dalm, R. H. Wijffels, D. E. Martens, *Cytotechnology* **2017**, *69*, 39.
- [25] K. Lin, H. Kools, P. J. de Groot, A. K. Gavai, R. K. Basnet, F. Cheng, J. Wu, X. Wang, A. Lommen, G. J. E. J. Hooiveld, G. Bonnema, R. G. F. Visser, M. R. Muller, J. a. M. Leunissen, *J. Integr. Bioinform.* **2011**, *8*, 160.
- [26] R. A. Irizarry, B. Hobbs, F. Collin, Y. D. Beazer-Barclay, K. J. Antonellis, U. Scherf, T. P. Speed, *Biostatistics* **2003**, *4*, 249.
- [27] M. Dai, P. Wang, A. D. Boyd, G. Kostov, B. Athey, E. G. Jones, W. E. Bunney, R. M. Myers, T. P. Speed, H. Akil, S. J. Watson, F. Meng, *Nucleic Acids Res.* **2005**, *33*, 1.
- [28] M. E. Ritchie, B. Phipson, D. Wu, Y. Hu, C. W. Law, W. Shi, G. K. Smyth, *Nucleic Acids Res.* **2015**, *43*, 7.
- [29] M. A. Sartor, C. R. Tomlinson, S. C. Wesselkamper, S. Sivaganesan, G. D. Leikauf, M. Medvedovic, *BMC Bioinform.* **2006**, *7*, 538.
- [30] I. H. Yuk, J. D. Zhang, M. Ebeling, M. Berrera, N. Gomez, S. Werz, C. Meiringer, Z. Shao, J. C. Swanberg, K. H. Lee, J. Luo, B. Szperalski, *Biotechnol. Prog.* **2015**, *31*, 1.
- [31] B. C. Mulukutla, M. Gramer, W. S. Hu, *Metab. Eng.* **2012**, *14*, 138.
- [32] D. B. Allison, X. Cui, G. P. Page, M. Sabripour, *Nat. Rev. Genet.* **2006**, *7*, 55.
- [33] T. Amann, A. H. Hansen, S. Kol, G. M. Lee, M. R. Andersen, H. F. Kildegaard, *Biotechnol. J.* **2018**, *1800122*, 1800111.
- [34] R. J. Marchant, M. B. Al-Fageeh, M. F. Underhill, A. J. Racher, C. M. Smales, *Mol. Biotechnol.* **2008**, *39*, 69.
- [35] H. Kaufmann, X. Mazur, M. Fussenegger, J. E. Bailey, *Biotechnol. Bioeng.* **1999**, *63*, 573.
- [36] S. Becerra, J. Berrios, N. Osses, C. Altamirano, *Biochem. Eng. J.* **2012**, *60*, 1.
- [37] N. S. Kim, G. M. Lee, *J. Biotechnol.* **2002**, *95*, 237.
- [38] J. X. Bi, J. Shuttlesworth, M. Al-Rubeai, *Biotechnol. Bioeng.* **2004**, *85*, 741.
- [39] Z. Du, D. Treiber, J. D. Mccarter, D. Fomina-Yadlin, R. A. Saleem, R. E. Mccoy, Y. Zhang, T. Tharmalingam, M. Leith, B. D. Follstad, B. Dell, B. Grisim, C. Zupke, C. Heath, A. E. Morris, P. Reddy, *Biotechnol. Bioeng.* **2015**, *112*, 141.
- [40] Y. Xu, L. R. Morse, R. A. B. da Silva, P. R. Odgren, H. Sasaki, P. Stashenko, R. A. Battaglini, *Antioxid. Redox Signal.* **2010**, *13*, 27.
- [41] N. Templeton, J. Dean, P. Reddy, J. D. Young, *Biotechnol. Bioeng.* **2013**, *110*, 2013.
- [42] F. Chen, X. Lin, P. Xu, Z. Zhang, Y. Chen, C. Wang, J. Han, B. Zhao, M. Xiao, X.-H. Feng, *Mol. Cell. Biol.* **2015**, *35*, 1700.
- [43] A. Satyanarayana, P. Kaldis, *Oncogene* **2009**, *28*, 2925.
- [44] F. Girard, U. Strausfeld, A. Fernandez, N. J. C. Lamb, *Cell* **1991**, *67*, 1169.
- [45] M. Ohtsubo, a M. Theodoras, J. Schumacher, J. M. Roberts, M. Pagano, *Mol. Cell. Biol.* **1995**, *15*, 2612.
- [46] O. Coqueret, *Trends Cell Biol.* **2003**, *13*, 65.
- [47] S. Y. Shieh, J. Ahn, K. Tamai, Y. Taya, C. Prives, *Genes Dev.* **2000**, *14*, 289.
- [48] J. Massague, R. S. Lo, *Cell* **2000**, *103*, 295.
- [49] M. B. Datto, Y. Li, J. F. Panus, D. J. Howe, Y. Xiong, X. F. Wang, *Proc. Natl. Acad. Sci. USA.* **1995**, *92*, 5545.
- [50] J. Massagué, *Nat. Rev. Mol. Cell Biol.* **2012**, *13*, 616.
- [51] M. H. Barcellos-Hoff, T. A. Dix, *Mol. Endocrinol.* **1996**, *10*, 1077.
- [52] Y. Qian, M. S. Rehmann, N.-X. Qian, A. He, M. C. Borys, P. S. Kayne, Z. J. Li, *Biotechnol. Bioeng.* **2018**, *115*, 1051.
- [53] R. M. Lyons, J. Keski-Oja, H. L. Moses, *J. Cell Biol.* **1988**, *106*, 1659.
- [54] Q. Yu, I. Stamenkovic, *Genes Dev.* **2000**, *14*, 163.
- [55] K. I. M. Jong Kyong, J. Alan Diehl, *J. Cell. Physiol.* **2009**, *220*, 292.
- [56] T. Schmelzle, M. N. Hall, *Cell* **2000**, *103*, 253.
- [57] J. D. Richter, N. Sonenberg, *Nature* **2005**, *433*, 477.
- [58] D. W. Lamming, D. M. Sabatini, *Cell Metab.* **2013**, *18*, 465.
- [59] T. Porstmann, C. R. Santos, B. Griffiths, M. Cully, M. Wu, S. Leever, J. R. Griffiths, Y. L. Chung, A. Schulze, *Cell Metab.* **2008**, *8*, 224.
- [60] D. C. Berwick, I. Hers, K. J. Heesom, S. Kelly Moule, J. M. Tavaré, *J. Biol. Chem.* **2002**, *277*, 33895.

- [61] J. J. Lum, D. E. Bauer, M. Kong, M. H. Harris, C. Li, T. Lindsten, C. B. Thompson, *Cell* **2005**, *120*, 237.
- [62] B. A. Hemmings, D. F. Restuccia, *Cold Spring Harb. Perspect. Biol.* **2012**, *4*, 011189.
- [63] V. Hwa, Y. Oh, R. G. Rosenfeld, *Acta Paediatrica* **1999**, *88*, 37.
- [64] T. F. Franke, C. P. Hornik, L. Segev, G. A. Shostak, C. Sugimoto, *Oncogene* **2003**, *22*, 8983.
- [65] X. M. Ma, J. Blenis, *Nat. Rev. Mol. Cell Biol.* **2004**, *5*, 827.
- [66] J. L. Jewell, R. C. Russell, K. Guan, *Nat. Rev. Mol. Cell Biol.* **2013**, *14*, 133.
- [67] B. C. Mulukutla, S. Khan, A. Lange, W.-S. Hu, *Trends Biotechnol.* **2010**, *28 VN-r*, 476.
- [68] C. Brancolini, M. Benedetti, C. Schneider, *EMBO J.* **1995**, *14*, 5179.
- [69] K. Nagai, T. Matsubara, A. Mima, E. Sumi, H. Kanamori, N. Iehara, A. Fukatsu, M. Yanagita, T. Nakano, Y. Ishimoto, T. Kita, T. Doi, H. Arai, *Kidney Int.* **2005**, *68*, 552.
- [70] G. Del Sal, M. E. Ruaro, L. Philipson, C. Schneider, *Cell* **1992**, *70*, 595.
- [71] B.-R. She, G.-G. Liou, S. Lin-Chao, *Exp. Cell Res.* **2002**, *273*, 34.
- [72] C. M. Smith, J. A. Steitz, *Mol. Cell. Biol.* **1998**, *18*, 6897.
- [73] C. Ma, X. Shi, Q. Zhu, Q. Li, Y. Liu, Y. Yao, Y. Song, *Tumor Biol.* **2016**, *37*, 1437.
- [74] E. Petroulakis, A. Parsyan, R. J. O. Dowling, O. LeBacquer, Y. Martineau, M. Bidinosti, O. Larsson, T. Alain, L. Rong, Y. Mamane, M. Paquet, L. Furic, I. Topisirovic, D. Shahbazian, M. Livingstone, M. Costa-Mattioli, J. G. Teodoro, N. Sonenberg, *Cancer Cell* **2009**, *16*, 439.
- [75] D. Fomina-Yadlin, J. J. Gosink, R. McCoy, B. Follstad, A. Morris, C. B. Russell, J. T. McGrew, *Biotechnol. Bioeng.* **2014**, *111*, 965.